Forschung im Ingenieurwesen 69 (2005) 170–180 © Springer-Verlag 2005
DOI 10.1007/s10010-005-0150-6

An anisotropic model of damage for brittle materials with different behavior in tension and compression

A. Zolochevsky, E. Yeseleva, W. Ehlers

Abstract The article outlines a continuum damage mechanics model for elastic deformation associated with the appearance and growth of parallel penny-shaped microcracks in brittle materials. The model is able to describe simultaneously the anisotropic nature of damage and the difference between the damaging processes under tensile and compressive loading types. Constitutive equation and damage evolution equations are developed on the basis of irreversible thermodynamic theory. Model parameters are determined from basic experiments formulated. The theoretical results are compared with the experimental data for two-dimensional stress states of gray cast iron.

Ein anisotropes Werkstoffmodell für spröde Werkstoffe mit unterschiedlichem Zug- und Druckverhalten

Zusammenfassung Der Artikel beschreibt ein kontinuummechanisches Schadensmodell für elastische Verformungen unter Berücksichtigung der Entstehung und des Wachstums von plättchen-förmigen Einschlüssen in spröden Werkstoffen. Das Modell beschreibt gleichzeitig das anisotrope Schadensverhalten und die verschiedenen Schadenbildungsprozesse unter Zug- und Druckbelastungen. Das zugehörige Werkstoffgesetz als auch die Schadensgleichungen beruhen auf der Theorie der irreversiblen Thermodynamik, wobei die notwendigen Modellparameter durch einfache Versuche bestimmt werden. Die theoretischen Ergebnisse werden experimentellen Daten für Grauguß unter zweiachsigen Spannungszuständen gegenübergestellt.

Received: 22. November 2004

A. Zolochevsky (✉)
Department of Materials Technology, Chemistry Block II,
Norwegian University of Science and Technology,
N-7491, Trondheim, Norway
e-mail: azol@rambler.ru

E. Yeseleva
Department of Mechanics,
Institute for Problems of Machinery,
Pozharsky 2/10, 61046, Kharkov, Ukraine

W. Ehlers
Institut für Mechanik (Bauwesen),
Universität Stuttgart, D-70569, Stuttgart, Germany

Support of the Alexander von Humboldt Stiftung (A.Z.) and of the DAAD (E.Y) is gratefully acknowledged.

List of symbols

Ω	Damage vector
n	Unit vector
ω	Scalar damage parameter
F	Gibbs specific enthalpy
σ	Cauchy stress tensor
ϵ	Strain tensor
$J_1, J_2, J_3, J_4, J_5, \bar{J}_5, J_6$	Joint invariants
I	Second order unit tensor
$\tau_e, \sigma_e, \Sigma_e$	Equivalent stresses
$\alpha, \beta, \gamma, \Psi, \kappa$	Weight coefficients
E, ν, G	Young's modulus, Poisson's ratio, elastic shear modulus
$A(\omega)$, $\bar{B}(\omega)$, $B(\omega)$, $C(\omega)$, $D(\omega)$, $K(\omega)$, $L(\omega)$, $M(\omega)$, $N(\omega)$, $P(\omega)$, $Q(\omega)$, $R(\omega)$, $U(\omega)$, $V(\omega)$	Some functions
$\sigma_1, \sigma_2, \sigma_3, \Sigma_1, \Sigma_2$	Polynomials
y_A, y_B, y_C	Thermodynamic forces
Z	Damage dissipation potential
λ	Damage consistency parameter
Σ_e^*	Damage threshold
Ψ	Function in the second thermodynamic principle
K_{IIC}, K_{IC}	Fracture toughnesses
A_0, B_0, C_0 , a, c	Material parameters
n, m, K_+, K_-, K_0	Material constants
E^+, E^-, G_{12}	Elastic secant moduli
γ_{12}	Shear strain under pure torsion

1 Introduction

Starting since papers of Kachanov [1] and Rabotnov [2], Continuum Damage Mechanics (CDM) was used in different areas of mechanics of solids including creep rupture, brittle and ductile failure, fatigue behavior. The aim of CDM is to describe the material degradation associated with the damage growth at the mesoscale level like appearance and growth of microcracks, microvoids, cavities and other microdefects, using continuum theories of mechanics of solids. A systematic consideration of the basic aspects of CDM can be found in monographs [3–11].

The elastic deformation of a large class of materials commonly termed «brittle» (rocks, ceramics, concretes, cast irons, some polymers) is related to the appearance of new microcracks and growth of already existing ones. The appearance of either microcrack mechanism depends on the material, type of the loading and environment. The

characteristic features of the damage growth in brittle materials may be investigated experimentally. Among these features are the following.

Firstly, an essential feature of the damage in brittle materials is the fact that microcracking occurs in some preferential directions. Usually, microdefects in brittle materials have the form of parallel penny-shaped microcracks that grow either in the cleavage mode or result from grain boundary sliding. Furthermore, in the uniaxial tension test the microcracks arise and grow mainly on planes that are nearly perpendicular to the load axis. The above analysis points out a directional nature of damage in brittle materials. Therefore, to describe the elastic deformation of brittle materials we must take into account an orientation dependent character of microcracks and damage-induced anisotropy.

Secondly, the progressive degradation of elastic properties reflecting damage growth in brittle materials strongly depends on the sign and magnitude of applied stresses. There are different mechanisms of microcracking under tension and compression. In tension, microcracks grow mostly in the interfacial zone between aggregate particles and binder which is the weakest link of the material mesostructure. These interfacial microcracks may develop due to the mix water migration during the forming process or due to the volume changes during hardening. As a result, microcracks grow perpendicular to the loading axis.

Otherwise, in compression the interaction between the various aggregate particles is the governing mechanism of microcracking in brittle materials. In this case, the particle interaction generates splitting tensile forces, causing vertical tensile microcracks in the interfacial zone. Therefore, tensile microcracking occurs even under global compressive stress, and thus, interfacial microcracks propagate along favourably oriented aggregate faces parallel to the loading axis. In very porous brittle materials, final fracturing by splitting takes place before frictional sliding occurs. In brittle materials with low porosity, frictional slip of microcracks surfaces can destabilize preexisting shear-type flaws, causing them to kink, and develop wing cracks. As a result in this case, final fracturing by shear crack mechanism takes place.

Furthermore, under multiaxial loading, microcracks arise and grow on planes more or less perpendicular to the maximum positive principal stress. This fact follows directly from the experimental data for two- and three-dimensional stress states of various brittle materials.

Thus, the characteristic features of brittle materials are the anisotropic nature of damage and the difference between the damaging processes under tensile and compressive loading types. These features lead to the fact that various brittle materials have different stress-strain diagrams in tension and compression [8, 12–17].

Let us return again to the analysis presented above that addresses the important issues of damage modeling. It is well known [9] that damage in materials may be active (open microcracks) and passive (closed microcracks). A microcrack subjected to a substantial compressive normal stress in the direction of its normal is a paradigm of a closed microcrack. In the case of uniaxial tension, microcracks perpendicular to the axis of tensile loading are open, and they affect elastic deformation. Otherwise, under uniaxial compression, microcracks perpendicular to the axis of compressive loading are closed, but preexisting microcracks parallel to this axis are open and affect elastic deformation. Of course, in the case of uniaxial compression, damage is still present but affects elastic deformation differently. Thus, we have two different damage states chosen for one and the same absolute value of stress (one in tension and the other in compression). In other words, there is the unilateral nature of damage [18, 19].

A more complex picture, which is related to the damage development, emerges during the process of nonproportional loading. Obviously, the damage state (active or passive) may change if the stress normal to the microcracks' plane changes its sign during loading. For example, under uniaxial tension, unloading and subsequent reverse loading in compression, the damage deactivation occurs. In this case, the crack closure phenomenon for preexisting microcracks takes place, and new microcrack nucleation occurs in the direction parallel to the loading axis.

Note also that there is no damage growth in brittle materials loaded by pure hydrostatic pressure. For example, the authors of [20] have not observed any penny-shaped microcracks under pure hydrostatic loading of the 30 rocks that they have examined with scanning electron microscopes. Furthermore, these authors have defined for each rock the hydrostatic pressure at which the preexisting microcracks close completely.

In the past 15 years, quite a large number of attempts to reproduce simultaneously damage induced anisotropy and unilateral damage in brittle materials have been made. A comprehensive review of these models until 1992 is given by Chaboche in [19]. The models existing in this direction since 1992 can be found in [12–15, 21–37]. In the most models under consideration, the idea of positive and negative stress and strain projection operators was used to account for tensile and compressive loading types.

The presence of various CDM models for brittle materials with different behavior in tension and compression for a definite level of knowledge about the influence of the kind of loading on the accumulating damage is apparently inevitable. Each new model introduces a certain addition to CDM for brittle materials whose elastic deformation depends on the kind of loading. Of course, extensive experimental confirmation of the proposed models is necessary.

The aim of this paper is to consider a new unilateral damage model for elastic deformation of brittle materials without using the concept of positive and negative projections of stress and strain tensors. In the following, small elastic strains in isothermal processes will be considered within the framework of the CDM at the mesoscale level. The approach proposed and substantiated in earlier papers [38–46] for the description of creep damage and fatigue damage in polycrystalline materials with different behavior in tension and compression will here be extended to the nonlinear elastic deformation of damaged materials. Taking into account that the development of modern CDM was started by the papers of Kachanov [1] and Rabotnov [2] in creep theory, it seems to be fruitful if the approach proposed earlier in [38–44] will be used for the description of elastic deformation for brittle materials with different

behavior in tension and compression. An experimental foundation of this approach for gray cast iron will be executed.

2
The formulation of a model

Let the elastic deformation of the initially isotropic brittle materials be accompanied by the nucleation and growth of parallel penny-shaped microcracks. A microcrack be any cavity within the brittle material that cannot seen without a microscope and that has an aspect ratio (cavity width divided by cavity length) less than 0.05. The coinciding orientation of the family of these parallel microcracks may be characterized by a unit vector n which may also be considered as damage normal. Then damage vector $\Omega = \omega \boldsymbol{n}$ may be introduced, where ω is the cumulative damage parameter ($\omega \geq 0$). According to Rabotnov [2], scalar damage parameter ω may be defined as the microcrack area density or net area reduction in the observed plane.

2.1
Elastic response

Taking into account the coupling between elasticity and damage, the Gibbs specific enthalpy F may be introduced as an invariant function of the Cauchy stress tensor σ and the dyadic product $\Omega \otimes \boldsymbol{n} = \omega \boldsymbol{n} \otimes \boldsymbol{n}$, i.e.

$$F = F(\sigma, \omega n \otimes n). \tag{1}$$

The integrity basis for the two symmetric second order tensors σ and $\omega n \otimes n$ consists of the following six irreducible invariants [40]

$$\begin{aligned} J_1 &= \text{ tr } \sigma = \sigma \cdot \cdot \boldsymbol{I}, \\ J_2 &= \text{ tr } \sigma^2 = \sigma_{ij}\sigma_{ij},\ J_3 = \text{ tr } \sigma^3 = \sigma_{ij}\sigma_{jk}\sigma_{ki}, \\ J_4 &= \text{ tr } (\omega \boldsymbol{n} \otimes \boldsymbol{n}) = \omega, \\ \bar{J}_5 &= \text{ tr } [(\omega \boldsymbol{n} \otimes \boldsymbol{n})\sigma] = \omega \boldsymbol{n} \cdot \sigma \cdot \boldsymbol{n} = \omega n_i \sigma_{ij} n_j, \\ J_6 &= \text{ tr } \left[(\omega \boldsymbol{n} \otimes \boldsymbol{n})\sigma^2\right] = \omega \boldsymbol{n} \cdot \sigma^2 \cdot \boldsymbol{n} = \omega n_i \sigma_{ij}\sigma_{jk} n_k. \end{aligned} \tag{2}$$

Here «tr» denotes the trace of a second order tensor, «.» denotes scalar product operation, and I is the second order unit tensor.

The invariants J_1 and J_2 are sufficient to describe the linear elastic deformation of the classical undamaged materials. In this case the Gibbs specific enthalpy is determined as

$$F = \frac{1}{2}\tau_e^2 \tag{3}$$

with the equivalent stress

$$\tau_e = \sqrt{aJ_1^2 + cJ_2}. \tag{4}$$

Material parameters a and c in (4) are related to the elastic modulus E and Poisson's ratio v by the relations

$$a = -\frac{v}{E}, \quad c = \frac{1+v}{E}. \tag{5}$$

In the case of nonlinear elastic deformation we assume the following structure for the Gibbs specific enthalpy

$$F = \frac{1}{2}\tau_e^2 + \frac{1}{2}\alpha\sigma_e^2, \tag{6}$$

where the equivalent stress σ_e has been introduced to describe the nonlinear deformation, and α is a weight coefficient taking into account the influence of the second term in the expression (6) for the thermodynamic potential. The representation (6) is a general form. For example, by placing $\alpha = 0$ in (6), we arrive at the classical linear elastic potential given by (3)–(5).

Let us define the equivalent stress σ_e ($\sigma_e \geq 0$). For this purpose, let us form the possible polynomials in terms of the stress tensor σ using all possible combinations from the integrity basis given by (2). In this direction, we can receive the linear

$$\sigma_1 = \overline{B}(\omega)\bar{J}_5 + \psi D(\omega)J_1, \tag{7}$$

quadratic

$$\sigma_2^2 = A(\omega)J_1 + C(\omega)J_2 + \beta K(\omega)J_1\bar{J}_5 + \gamma L(\omega)J_6 \tag{8}$$

and cubic

$$\begin{aligned} \sigma_3^3 = {} & M(\omega)J_1^3 + N(\omega)J_1J_2 + P(\omega)J_1J_6 \\ & + Q(\omega)\bar{J}_5^3 + R(\omega)J_2\bar{J}_5 + U(\omega)\bar{J}_5J_6 + V(\omega)J_3. \end{aligned} \tag{9}$$

polynomials, where $A(\omega)$, $\bar{B}(\omega)$, $C(\omega)$, $D(\omega)$, $K(\omega)$, $L(\omega)$, $M(\omega)$, $N(\omega)$, $P(\omega)$, $Q(\omega)$, $R(\omega)$, $U(\omega)$ and $V(\omega)$ are some functions of the cumulative damage parameter, β, γ and ψ are weight coefficients taking into account the influence of different terms in the polynomials. Considering the equivalent stress σ_e as a homogeneous function of the stresses, we can assume that

$$\sigma_e = \sigma_1 + \sigma_2 + \kappa\sigma_3, \tag{10}$$

where κ is a weight coefficient taking into account the influence of the function σ_3 in the representation (10).

The proposed expression (10) is quite general, and its application for the description of the elastic deformation is very complicated. Otherwise, as known from [8, 38, 47], the simpler structure for the equivalent stress in the case of materials with different properties in tension and compression must be related to three independent damage functions and three irreversible invariants. In this regard, neglecting the influence of the invariants J_1, $J_1\bar{J}_5$, J_6 and the cubic polynomial in the expression (10) for the equivalent stress as second order effects we put in (7)–(10)

$$\beta = \gamma = \psi = \kappa = 0. \tag{11}$$

Thus, we obtain the following structure for the equivalent stress

$$\sigma_e = \sigma_1 + \sigma_2 \tag{12}$$

with

$$\sigma_1 = B(\omega)J_5 \tag{13}$$

and

$$\sigma_2^2 = A(\omega)J_1^2 + C(\omega)J_2, \tag{14}$$

where, for convenience, new invariant

$$J_5 = tr[(\boldsymbol{n} \otimes \boldsymbol{n})\sigma] = \boldsymbol{n} \cdot \sigma \cdot \boldsymbol{n} = n_i\sigma_{ij}n_j \tag{15}$$

is introduced, and $B(\omega)$ is some function of the cumulative damage parameter.

The thermodynamic internal force associated with the state variable σ (i.e. the elastic infinitesimal strain tensor ε) can be determined by the rule

$$\varepsilon = \frac{\partial F}{\partial \sigma}. \tag{16}$$

Therefore, using (2), (4), (6), (12)–(15) and the relations

$$\begin{aligned} &\frac{\partial F}{\partial \sigma} = \tau_e \frac{\partial \tau_e}{\partial \sigma} + \alpha \sigma_e \left(\frac{\partial \sigma_1}{\partial \sigma} + \frac{\partial \sigma_2}{\partial \sigma} \right), \\ &\frac{\partial \tau_e}{\partial \sigma} = \frac{a J_1 \boldsymbol{I} + c\sigma}{\tau_e}, \quad \frac{\partial \sigma_1}{\partial \sigma} = B(\omega) \boldsymbol{n} \otimes \boldsymbol{n}, \\ &\frac{\partial \sigma_2}{\partial \sigma} = \frac{A(\omega) J_1 \boldsymbol{I} + C(\omega)\sigma}{\sigma_2} \end{aligned} \tag{17}$$

we arrive at the constitutive equation

$$\varepsilon = a J_1 \boldsymbol{I} + c\sigma + \alpha \sigma_e \left[B(\omega) \boldsymbol{n} \otimes \boldsymbol{n} + \frac{A(\omega) J_1 \boldsymbol{I} + C(\omega)\sigma}{\sigma_2} \right] \tag{18}$$

of elastic deformation for brittle damaged materials with different behavior in tension and compression.

2.2
Damage evolution equations

The Gibbs specific enthalpy F associated with the present state can be considered as a function of the stress tensor σ and the three damage variables $A = A(\omega)$, $B = B(\omega)$, $C = C(\omega)$. Then the three forces associated with these damage variables are, respectively, given by

$$y_A = \frac{\partial F}{\partial A}, \quad y_C = \frac{\partial F}{\partial C}, \quad y_B = \frac{\partial F}{\partial B}. \tag{19}$$

Therefore, using (2), (4), (6), (12)–(15) we obtain

$$y_A = \frac{1}{2} \frac{\sigma_e}{\sigma_2} J_1^2, \quad y_C = \frac{1}{2} \frac{\sigma_e}{\sigma_2} J_2, \quad y_B = \sigma_e J_5. \tag{20}$$

Let us consider the new polynomials

$$\Sigma_1 = B_0 J_5 \tag{21}$$

and

$$\Sigma_2^2 = A_0 J_1^2 + C_0 J_2 \tag{22}$$

on the basis of the invariants J_1, J_2 and J_5, and material parameters A_0, B_0 and C_0. Then we can introduce the following structure for the damage dissipation potential

$$Z = \sigma_e (\Sigma_1 + 2\Sigma_2). \tag{23}$$

Then using (20)–(22) it is not difficult to rewrite (23) as

$$Z = B_0 y_B + 2\sqrt{2\sigma_e \sigma_2 \left(A_0 y_A + C_0 y_C \right)}. \tag{24}$$

The damage process is described by the following equations of evolution

$$\dot{A} = \dot{\lambda} \frac{\partial Z}{\partial y_A}, \quad \dot{C} = \dot{\lambda} \frac{\partial Z}{\partial y_C}, \quad \dot{B} = \dot{\lambda} \frac{\partial Z}{\partial y_B}, \tag{25}$$

where the dot above symbol denotes the derivative with respect to time, and λ is the damage consistency parameter which can be considered as a measure of the cumulative damage, i.e.

$$\dot{\lambda} = \dot{\omega}. \tag{26}$$

Thus, (24)–(26) furnish the following damage evolution equations:

$$\dot{A} = 2\dot{\omega} \frac{\sigma_2}{\Sigma_2} A_0, \quad \dot{C} = 2\dot{\omega} \frac{\sigma_2}{\Sigma_2} C_0, \quad \dot{B} = \dot{\omega} B_0. \tag{27}$$

Let us consider the evolution equation for the cumulative damage parameter. For example, in the case of brittle materials without softening we can introduce the equivalent stress in the damage description as

$$\Sigma_e = \Sigma_1 + \Sigma_2 \tag{28}$$

and we can use a power law to relate increments in the damage parameter ω to current values of Σ_e and their increments:

$$\frac{d\omega}{d\Sigma_e} = \begin{cases} n(\sqrt{\alpha})^n \left(\Sigma_e - \Sigma_e^* \right)^{n-1} & \text{if } \Sigma_e > \Sigma_e^* \text{ and } \dot{\Sigma}_e > 0 \\ 0 \quad \text{if } \Sigma_e \le \Sigma_e^*, \text{ or } \Sigma_e > \Sigma_e^* \text{and } \dot{\Sigma}_e \le 0 \end{cases} \tag{29}$$

where n is a material constant, Σ_e^* is the threshold below which no damage occurs. In the case of brittle materials with softening the evolution equation for ω can be formulated using the recommendations obtained in [15, 48]. Further discussion of this issue is considered to be beyond the scope of the present paper.

Thus, the damage development in brittle materials with different behavior in tension and compression is described by (27) and (29). These evolution equations must be considered together with constitutive equation (18) for elastic deformation.

2.3
The second thermodynamic principle

Let us analyze the validity of the second thermodynamic principle for the damage model under consideration. Obviously, the second thermodynamic principle uses the following expression [5]

$$\Psi = y_A \dot{A} + y_C \dot{C} + y_B \dot{B}. \tag{30}$$

Substituting the values in (20) and (27) into (30) and using (28), we obtain

$$\Psi = \dot{\omega} \sigma_e \Sigma_e. \tag{31}$$

Now we see that under the natural conditions the cumulative damage parameter is a non-decreasing function of time (i.e. $\dot{\omega} \ge 0$) and the equivalent stress is always non-negative (i.e. $\sigma_e \ge 0$ and $\Sigma_e \ge 0$), the second thermodynamic principle $\Psi \ge 0$ is always valid.

3
Basic experiments

Let us consider the determination of model parameters. In this regard, we use the results of basic experiments under uniaxial tension, uniaxial compression and pure torsion on standard specimens made from brittle materials without softening. Comparatively, we shall use Eqs. (18), (27) and (29) of the proposed model. We shall also assume that microcracks in brittle materials are always orthogonal to the direction of the maximum principal stress. Thus, we

shall consider an approach motivated by the Mode I microcrack opening and closing mechanism and characterized by microcracks distribution in brittle materials with much smaller fracture toughness K_{IIC} when comparing with the analogous magnitude K_{IC}. We shall not consider the case when a microcrack kinks out of its original plane and the tip of the secondary microcrack follows a path that is perpendicular to the maximum hoop stress.

3.1 Uniaxial tension

In the case of uniaxial tension we have the following strain in the direction of loading

$$\varepsilon_{11} = \frac{\sigma_{11}}{E^+}, \tag{32}$$

where σ_{11} is the magnitude of the corresponding tensile stress, and E^+ is the elastic secant modulus in tension.

Otherwise, under uniaxial tension microcracks form and propagate perpendicular to the axis of tensile loading. Therefore, the damage direction is represented by the vector $\boldsymbol{n} = [1, 0, 0]^{\mathrm{T}}$. Integrating then (27) and using (5) and (18), we obtain

$$\varepsilon_{11} = \left[\frac{1}{E} + \alpha\omega^2\left(\sqrt{A_0 + C_0} + B_0\right)^2\right]\sigma_{11}. \tag{33}$$

Comparing (32) and (33), the expression for the cumulative damage parameter can be derived as

$$\omega = \frac{\left(\frac{1}{E^+} - \frac{1}{E}\right)^{\frac{1}{2}}}{\sqrt{\alpha}\left(\sqrt{A_0 + C_0} + B_0\right)}. \tag{34}$$

Let the stress-strain diagram in uniaxial tension can be approximated by the expression

$$\varepsilon_{11} = \frac{\sigma_{11}}{E} + K_+\sigma_{11}^m, \tag{35}$$

where K_+ and m are some material constants.

Assuming no damage threshold we can adopt

$$\Sigma_e^* = 0, \quad n = \frac{1}{2}(m - 1) \tag{36}$$

Integrating then (29) we have

$$\omega = \left[\sqrt{\alpha}\left(\sqrt{A_0 + C_0} + B_0\right)\right]^n \sigma_{11}^n. \tag{37}$$

Using then (33), (35)–(37), we obtain

$$\sqrt{\alpha}\left(\sqrt{A_0 + C_0} + B_0\right) = K_+^{\frac{1}{m+1}}. \tag{38}$$

3.2 Uniaxial compression

The strain in the direction of the uniaxial compressive loading can be given by the expression

$$\varepsilon_{11} = -\frac{|\sigma_{11}|}{E^-}, \tag{39}$$

where σ_{11} is the magnitude of the corresponding compressive stress, and E^- is the elastic secant modulus in compression.

Taking into account that under uniaxial compression microcracks run parallel to the axis of loading, the orientation of the family of microcracks is represented by the vector $\mathrm{n} = [0, 1, 0]^{\mathrm{T}}$. By integrating (27), we obtain from (18) that

$$\varepsilon_{11} = -\left[\frac{1}{E} + \alpha\omega^2\left(\sqrt{A_0 + C_0}\right)^2\right]|\sigma_{11}|. \tag{40}$$

Comparing then (39) and (40), it is not difficult to write the following expression for the cumulative damage parameter

$$\omega = \frac{\left(\frac{1}{E^-} - \frac{1}{E}\right)^{\frac{1}{2}}}{\sqrt{\alpha}\sqrt{A_0 + C_0}}. \tag{41}$$

It is seen from (41) that $\omega = 0$ during linear deformation, and after that this damage parameter is a monotonically increasing function.

Let the elastic response in uniaxial compression can be described by the relation

$$\varepsilon_{11} = -\left(\frac{|\sigma_{11}|}{E} + K_-|\sigma_{11}|^m\right), \tag{42}$$

where K_- and m are some material constants ($K_- > 0$). Then, it follows from (29) and (36) that

$$\omega = \left[\sqrt{\alpha}\left(\sqrt{A_0 + C_0}\right)\right]^n |\sigma_{11}|^n. \tag{43}$$

Using (40), (42) and (43), it is not difficult to obtain

$$\sqrt{\alpha}\sqrt{A_0 + C_0} = K_-^{\frac{1}{m+1}}. \tag{44}$$

3.3 Pure torsion

For pure torsion we can use the following relation between the magnitude of the shear strain γ_{12} and the magnitude σ_{12} of the shear stress

$$\gamma_{12} = \frac{\sigma_{12}}{G_{12}}, \tag{45}$$

where G_{12} is the secant shear modulus.

Note also that in the case of pure torsion microcracks in a material propagate at an angle of $\pi/4$ with respect to axes 1, 2. Therefore, we have

$$n = \left[\frac{1}{\sqrt{2}}, \frac{1}{\sqrt{2}}, 0\right]^T. \tag{46}$$

By an analogous procedure under uniaxial tension and uniaxial compression, in the case of pure torsion it follows that

$$\gamma_{12} = -\left[\frac{1}{G} + \alpha\omega^2\left(\sqrt{2C_0} + B_0\right)\right]\sigma_{12} \tag{47}$$

and

$$\omega = \frac{\left(\frac{1}{G_{12}} - \frac{1}{G}\right)^{\frac{1}{2}}}{\sqrt{\alpha}\left(\sqrt{2C_0} + B_0\right)}. \tag{48}$$

Let the elastic response in pure torsion can be described by the relation

$$\gamma_{12} = \frac{\sigma_{12}}{G} + K_0 \sigma_{12}^m, \tag{49}$$

where G is the modulus of elasticity in shear of the material, $G = \frac{E}{2(1+\nu)}$, K_0 and m are some material constants.

Then, it follows from (29) and (36) that

$$\omega = \left[\sqrt{\alpha}\left(\sqrt{2C_0} + B_0\right)\right]^n \sigma_{12}^n. \tag{50}$$

Using then (48), (49) and (50), we obtain

$$\sqrt{\alpha}\left(\sqrt{2C_0} + B_0\right) = K_0^{\frac{1}{m+1}}. \tag{51}$$

3.4
Determination of material parameters

Using (38), (44) and (51) it is not difficult to obtain

$$\begin{aligned} \sqrt{\alpha} B_0 &= K_+^{\frac{1}{m+1}} - K_-^{\frac{1}{m+1}}, \\ \sqrt{2\alpha C_0} &= K_0^{\frac{1}{m+1}} - \sqrt{\alpha} B_0, \\ \alpha A_0 &= K_-^{\frac{2}{m+1}} - \alpha C_0 \end{aligned} \tag{52}$$

4
Comparison of experimental and theoretical results

Let us consider the experimental data for gray cast iron [49]. We firstly discuss the results of basic experiments in uniaxial tension, uniaxil compression and pure torsion represented in Figs. 1–3, respectively. Different experimental values are given here for the nonlinear deformation ε_{11} related to different values of the normal stress σ_{11} in the case of uniaxial tension and uniaxial compression as well as for shear deformation γ_{12} related to different values of the shear stress σ_{12} in the case of pure torsion (symbol 'x'). Analyzing the linear elastic behavior of gray cast iron, we are establishing the independence of the characteristics on the kind of loading, and we are determining the elastic constants of the material: the Young's modulus $E = 107$ GPa and the shear modulus $G = 44$ GPa. Furthermore, considering the nonlinear elastic deformation, we see the possibility of using (38), (44) and (51) and we find the constants

$$\begin{aligned} &m = 4.4, K_+ = 1.53 \cdot 10^{-(8+m)} \text{ Mpa}^{-m}, \\ &K_- = 8.1 \cdot 10^{-(10+m)} \text{ Mpa}^{-m}, \\ &K_0 = 9.07 \cdot 10^{-(8+m)} \text{ Mpa}^{-m}. \end{aligned} \tag{53}$$

Thus, it can be seen that the given isotropic material shows the different behavior in tension and compression as well as the independent law of the deformation under the

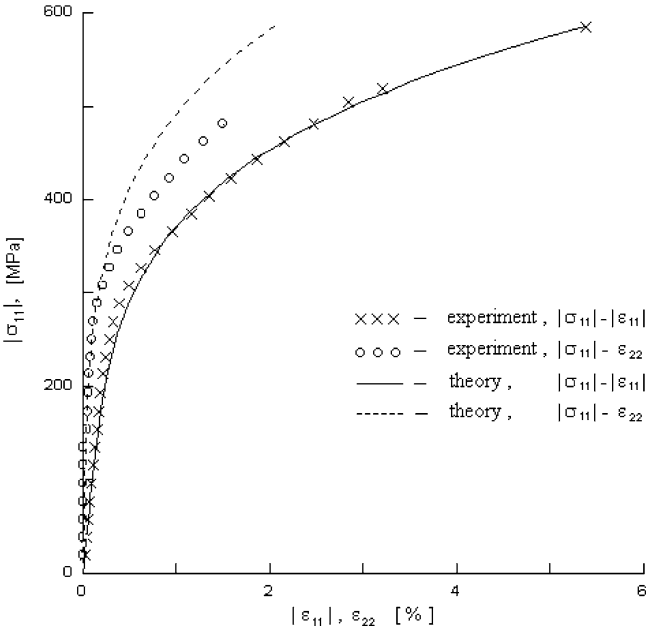

Fig. 2. Stress–strain diagrams for uniaxial compression

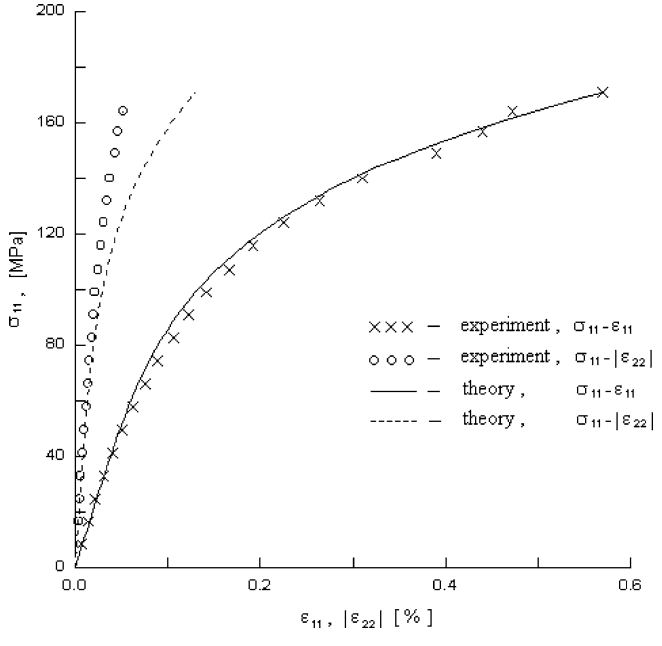

Fig. 1. Stress–strain diagrams for uniaxial tension

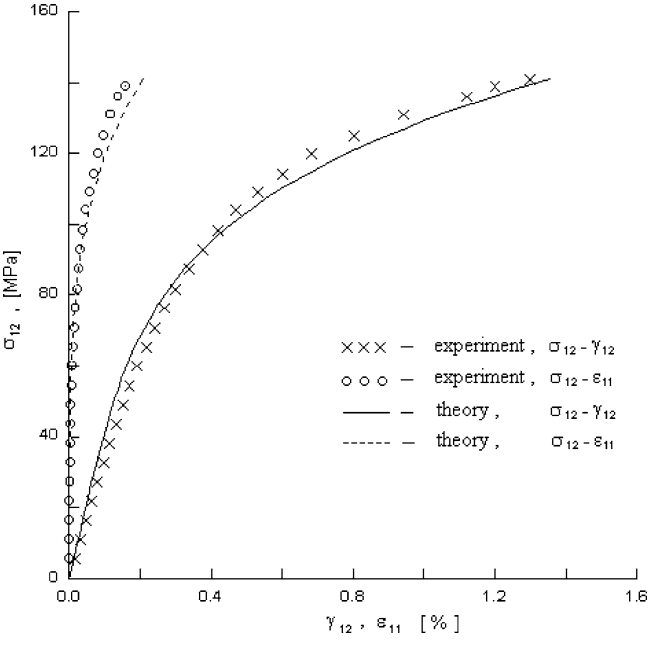

Fig. 3. Stress–strain diagrams for pure torsion

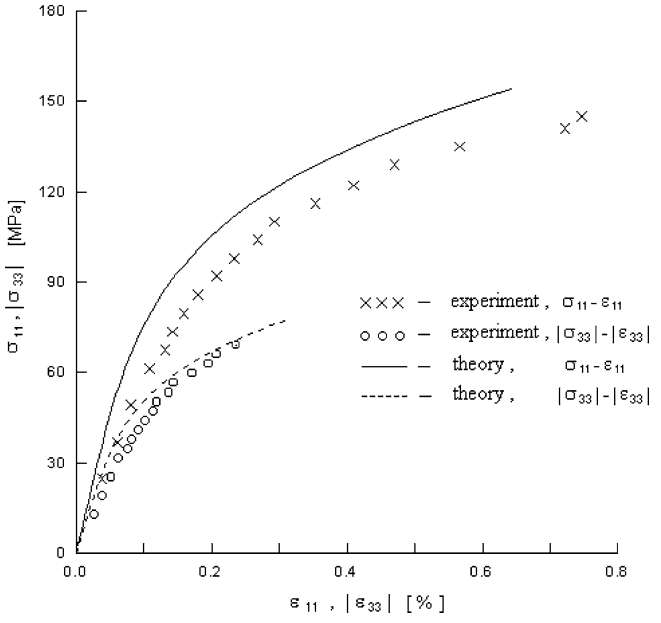

Fig. 4. Stress–strain diagrams for combined tension and torsion with $\sigma_{11}/|\sigma_{33}| = 2$

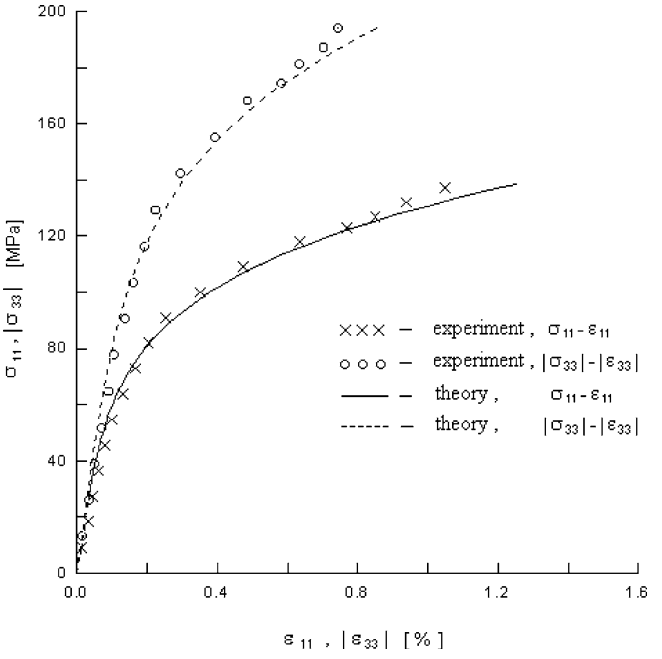

Fig. 6. Stress–strain diagrams for combined compression and torsion with $|\sigma_{33}|/\sigma_{11} = 1.4$

conditions of pure torsion. Presented in Figs. 1–3 solid lines are the results of calculations on the basis of the above-mentioned dependences (33), (40), (47) and material constants given in (53), while the experimental data are denoted by symbol 'x'.

Here and in the following we assume that microcracks in gray cast iron are always orthogonal to the direction of the maximum principal stress.

Let us then consider the experimental data for a complex stress state. The results of tests on thin-walled tubular specimens of the same material loaded by an axial (tensile or compressive) force and a torque are represented in Figs. 4–9 for the principal directions in the form of the dependences $\sigma_{11} - \varepsilon_{11}$ (symbol 'x') and $\sigma_{33} - \varepsilon_{33}$ (symbol 'o'). Here, σ_{11} is the maximum principal stress, σ_{33} is the minimum principal stress, $\sigma_{22} = 0$. The experimental data for thin-walled tubular specimens from gray cast iron subjected to internal pressure and axial load (biaxial tension) are presented in Figs. 10,11 in the form of the rela-

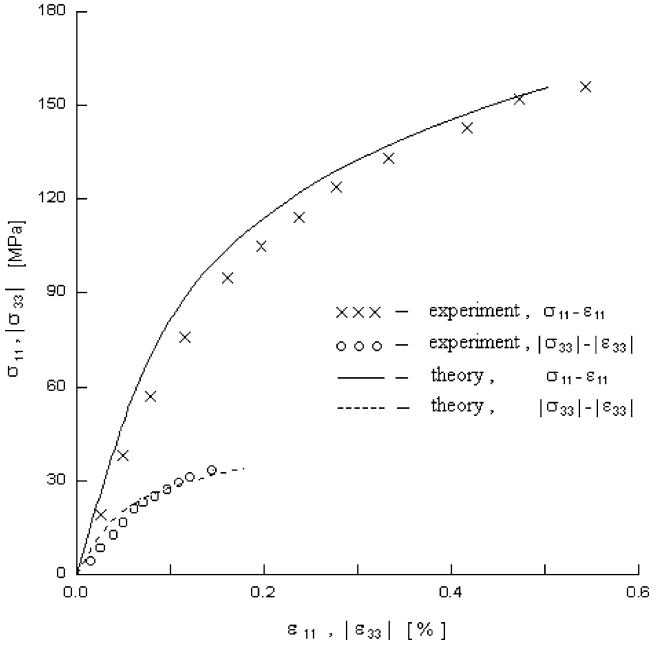

Fig. 5. Stress–strain diagrams for combined tension and torsion with $\sigma_{11}/|\sigma_{33}| = 4.6$

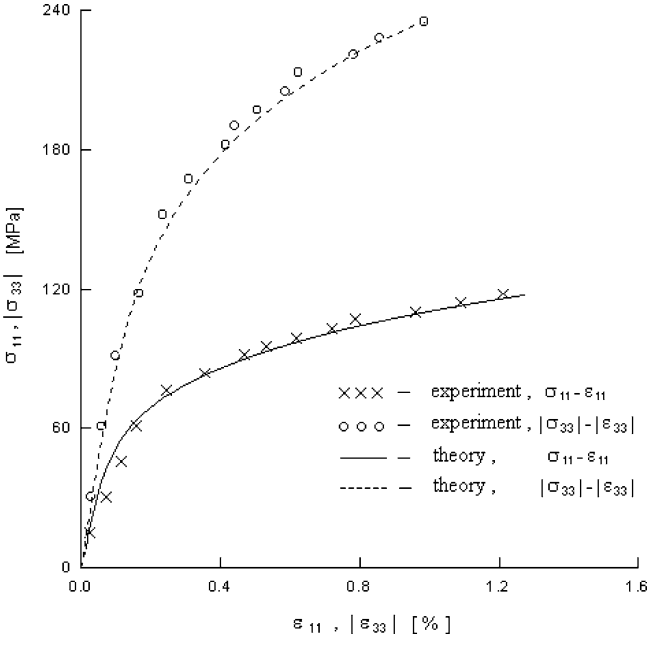

Fig. 7. Stress–strain diagrams for combined compression and torsion with $|\sigma_{33}|/\sigma_{11} = 2$

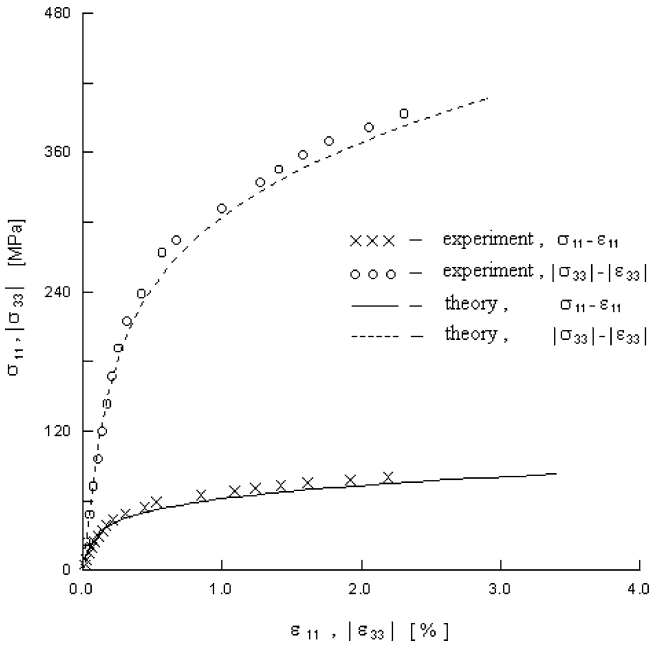

Fig. 8. Stress–strain diagrams for combined compression and torsion with $|\sigma_{33}|/\sigma_{11} = 4.9$

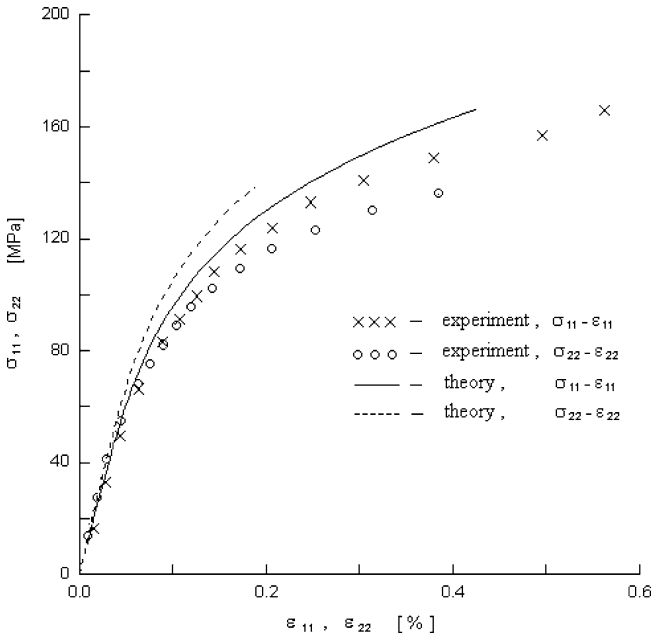

Fig. 10. Stress–strain diagrams for biaxial tension with $\sigma_{11}/\sigma_{22} = 1.2$

tions $\sigma_{11} - \varepsilon_{11}$ (symbol 'x') and $\sigma_{22} - \varepsilon_{22}$ (symbol 'o'). In this case σ_{11} is the axial stress in the specimen, and σ_{22} is the circumferential stress.

The solid and dashed lines in Figs. 4–11 are the appropriate theoretical curves based on Eqs. (18), (27) and (29). Here the solid lines correspond to the dependences $\sigma_{11} - \varepsilon_{11}$ while the dashed lines correspond to the dependences $\sigma_{33} - \varepsilon_{33}$ (Figs. 4–9) and the dependences $\sigma_{22} - \varepsilon_{22}$ (Figs. 10, 11). We can see the satisfactory agreement between the experimental data and theoretical results that gives a foundation for the possibility of using the proposed damage model.

Note also that the damage model under consideration predicts satisfactory transverse strains under uniaxial tension and under uniaxial compression as well as axial strains in conditions of pure torsion. The dashed lines in Figs. 1–3 are the appropriate theoretical curves while the analogous experimental data are denoted by circles.

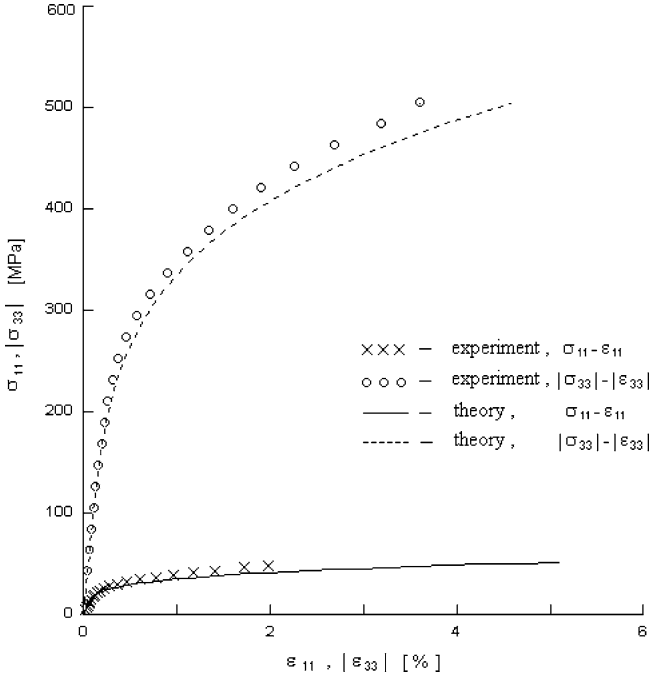

Fig. 9. Stress–strain diagrams for combined compression and torsion with $|\sigma_{33}|/\sigma_{11} = 9.4$

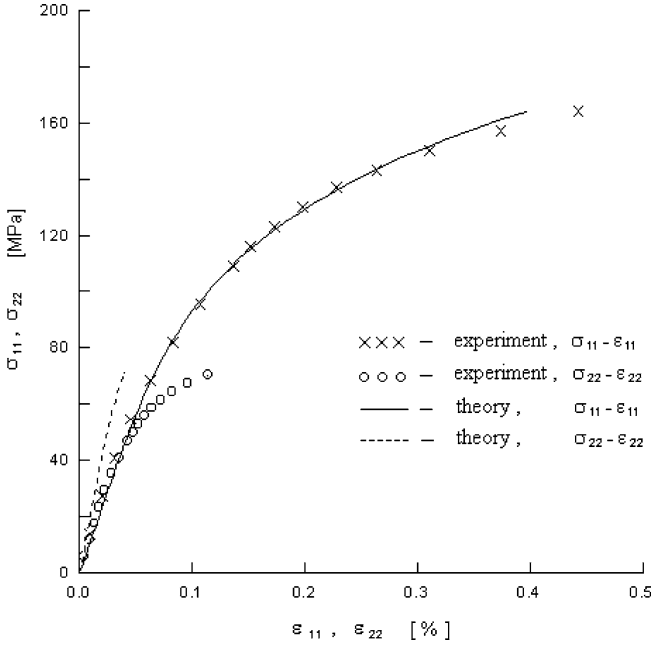

Fig. 11. Stress–strain diagrams for biaxial tension with $\sigma_{11}/\sigma_{22} = 2.3$

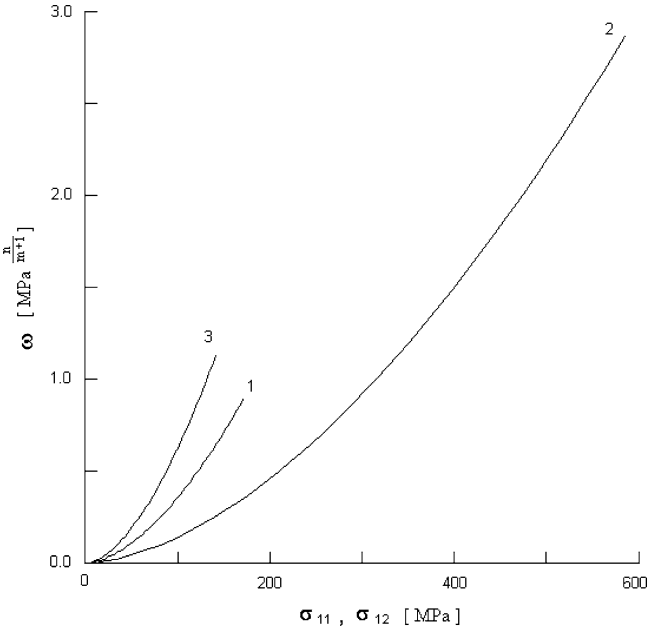

Fig. 12. Damage development under uniaxial tension (1), uniaxial compression (2) and pure torsion (3)

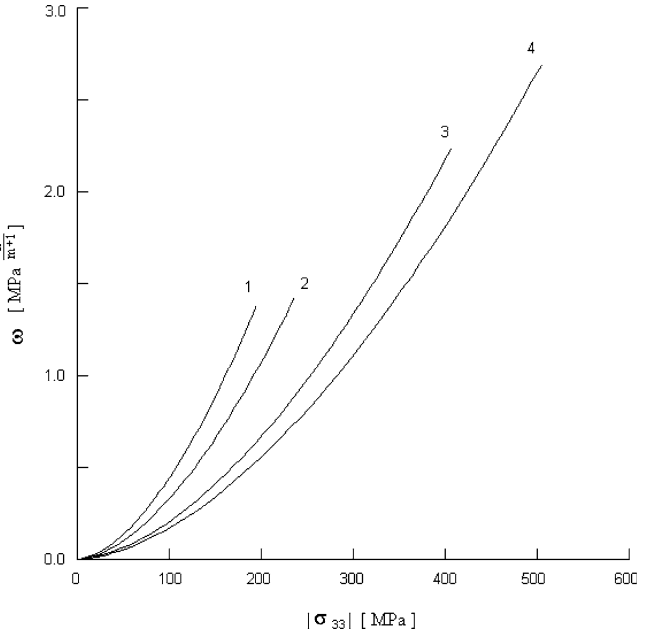

Fig. 14. Damage growth for combined compression and torsion: 1 – $|\sigma_{33}|/\sigma_{11} = 1.4$; 2 – $|\sigma_{33}|/\sigma_{11} = 2$; 3 – $|\sigma_{33}|/\sigma_{11} = 4.9$; 4 – $|\sigma_{33}|/\sigma_{11} = 9.4$

Figures. 12–15 illustrate the damage growth under elastic deformation of gray cast iron in basic experiments as well as under multiaxial loading. It is seen the features of the influence of the level and kind of loading on the damage evolution. For example, as can be seen in Fig. 12, at the same absolute value of the stress intensity the cumulative damage parameter is largest under uniaxial tension and smallest under uniaxial compression.

5 Conclusions

A new unilateral damage model for elastic deformation of brittle materials without using the concept of positive and negative projections of stress and strain tensor is proposed. Damage in the materials under consideration is associated with the elastic deformation, and nucleation and growth of parallel flat microcracks. The damage vectors associated with parallel flat microcracks and cumulative damage parameter are introduced to account for the

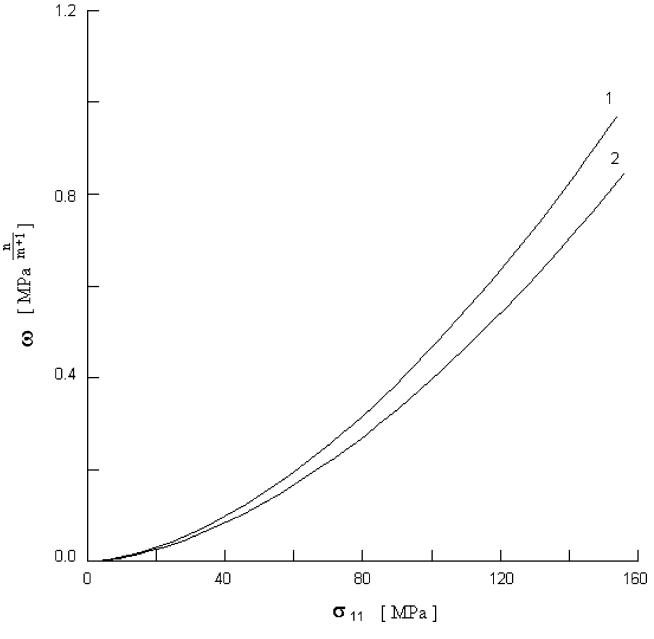

Fig. 13. Damage growth for combined tension and torsion: 1 – $\sigma_{11}/|\sigma_{33}| = 2$; 2 – $\sigma_{11}/|\sigma_{33}| = 4.6$

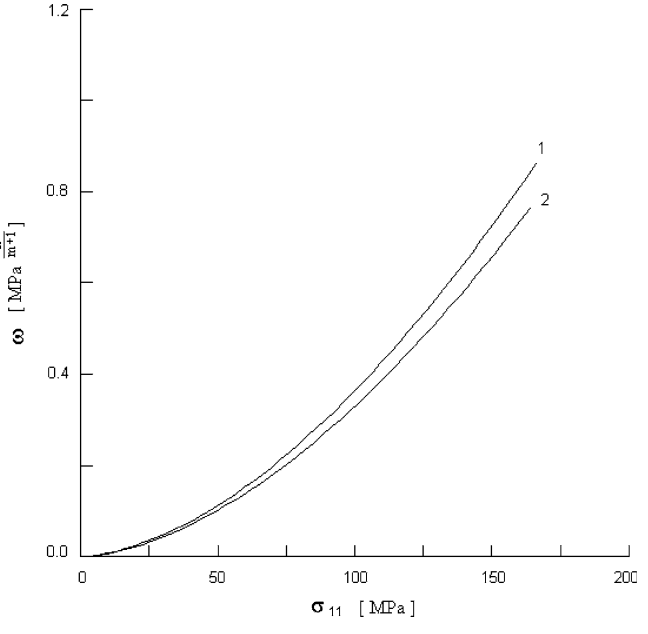

Fig. 15. Damage growth in specimens subjected to internal pressure and tensile load: 1 – $\sigma_{11}/\sigma_{22} = 1.2$; 2 – $\sigma_{11}/\sigma_{22} = 2.3$

damage under elastic deformation. The classical thermodynamics of irreversible processes is used to describe different damage development in tension and compression, and damage induced anisotropy. The constitutive equation for elastic deformation and equation for cumulative damage evolution are derived. The theoretical results have been compared with the experimental results under uniaxial and multiaxial loading. The model parameters are first determined from basic experiments under uniaxial tension, uniaxial compression, and pure torsion. Then a good correlation is obtained between the results generated from the model and the experimental data on thin-walled tubular specimens subjected to an axial (tensile or compressive) force together with a torque, and loaded by internal pressure and an axial load. The material under consideration is gray cast iron.

References

1. **Kachanov LM** (1958) On the time to failure under creep conditions. Izv. AN SSSR Otd. Tekhn. Nauk (8), 26–31
2. **Rabotnov Yu N** (1959) On the mechanism of long-term failure. In: Problems of Strength for Materials and Structures, 5–7, AN SSSR, Moscow
3. **Kachanov LM** (1986) Introduction to continuum damage mechanics. M. Nijhoff, Dordrecht
4. **Rabotnov Yu N** (1969) Creep problems in structural members. North-Holland, Amsterdam
5. **Lemaitre J, Chaboche JL** (1990). Mechanics of solid materials. Cambridge University Press, Cambridge
6. **Lemaitre J** (1992) A course on damage mechanics. Springer, Berlin
7. **Betten J** (2002) Creep mechanics. Springer, Berlin
8. **Altenbach H, Altenbach J, Zolochevsky A** (1995) Erweiterte Deformationsmodelle und Versagenskriterien der Werkstoffmechanik. Deutscher Verlag für Grundstoffindustrie, Stuttgart
9. **Krajcinovic D** (1996) Damage mechanics. Elsevier, Amsterdam
10. **Skrzypek J, Ganczarski A** (1998) Modeling of damage and creep failure of structures. Springer, Berlin
11. **Voyiadjis GZ, Kattan PI** (1999) Advances in damage mechanics: metals and metal matrix composites. Elsevier Science, Amsterdam
12. **Ladeveze P, Gasser A, Allix O** (1994) Damage mechanics modeling for ceramics composites. Trans. ASME J. Eng. Mat. Tech. 116, 331–336
13. **Shan H-Z, Pluvinage P, Parvizi-Majidi A, Chou T-W** (1994) Damage mechanics of two- dimensional woven SIC/SIC composites. Trans. ASME J. Eng. Mat. Tech. 116, 403–407
14. **Chaboche JL, Lesne PM, Maire JF** (1995) Continuum damage mechanics, anisotropy and damage deactivation for brittle materials like concrete and ceramic composites. Int. J. Damage Mech. 4, 5–22
15. **Lubarda VA, Krajcinovic D, Mastilovic S** (1994) Damage model for brittle elastic solids with unequal tensile and compressive strength. Eng. Fracture Mech. 49, 681–697
16. **Yazdani S, Schreyer HL** (1988) An anisotropic damage model with dilatation for concrete. Mech. Mater. 7, 231–244
17. **Van Mier JGM, Schlangen E, Vervuurt A, Van Vliet MRA** (1995) Damage analysis of brittle disordered materials: concrete and rock. In: Mechanical Behaviour of Materials: Invited Lectures of the 7th International Conference (ICM-7), 101–126, Delft University Press, Delft.
18. **Lemaitre J** (1987) Formulation and identification of damage kinetic constitutive equations. In: Krajcinovic D, Lemaitre J (eds), Continuum Damage Mechanics. Theory and Applications (CISM Courses and Lectures, No 295), 37–89, Springer, Wien
19. **Chaboche JL** (1992) Damage induced anisotropy: On the difficulties associated with the active/passive unilateral condition. Int. J. Damage Mech. 1, 148–171
20. **Stiegfried R, Simmons G** (1978) Characterization of oriented cracks with differential strain analysis. J. Geoph. Research. 83, 1269–1278
21. **Stevens DJ, Liu D** (1992) Strain-based constitutive model with mixed evolution rules for concrete. J. Eng. Mech. 118, 1184–1200
22. **Hansen NR, Schreyer HL** (1992) Deactivation of damage effects. In: Ju J W (ed), Recent Advances in Damage Mechanics and Plasticity, 63–76, AMD 132, ASME
23. **Chaboche JL** (1993) Development of continuum damage mechanics for elastic solids sustaining anisotropic and unilateral damage. Int. J. Damage Mech. 2, 311–329
24. **Gambarotta L, Lagomarsino S** (1993) A microcrack damage model for brittle materials. Int. J. Solids Struct. 30, 177–198
25. **Yazdani S** (1993) On a class of continuum damage mechanics theories. Int. J. Damage Mech. 2, 162–176
26. **Dragon A, Cormery F, Desoyer T, Halm D** (1994) Localized failure analysis using damage models. In: Chambon R (ed.), Localization and Bifurcation Theory for Solids and Rocks, 127–140, Balkema, Rotterdam
27. **Gerard A, Baste S** (1994) A constitutive relation for microcracked materials including the effects of microcrack opening-closing. Int. J. Eng. Sci. 32, 557–567
28. **Curnier A, He Q, Zysset, P** (1995) Conewise linear elastic materials. J. Elasticity. 37, 1–38
29. **Govindjee S, Kay G, Simo J** (1995) Anisotropic modelling and numerical simulation of brittle damage in concrete. Int. J. Num. Meth. Eng. 38, 3611–3633
30. **Halm D, Dragon A** (1996) A model of anisotropic damage by mesocrack growth; unilateral effect. Int. J. Damage Mech. 5, 384–402
31. **Fremond M, Nedjar B** (1996) Damage, gradient of damage and principle of virtual power. Int. J. Solids Struct. 33, 1083–1103
32. **Yazdani S, Karnawat S** (1997) Mode I damage modeling in brittle preloading. Int. J. Damage Mech. 6, 153–165
33. **Murakami S, Kamiya K** (1997) Constitutive and damage evolution equations of elastic-brittle materials based on irreversible thermodynamics. Int. J. Mech. Sci. 39, 473–486
34. **Halm D, Dragon A** (1998) An anisotropic model of damage and frictional sliding for brittle materials. Eur. J. Mech. A/Solids. 17, 439–460
35. **Betten J, Zolochevska L, Zolochevsky A** (1999) Modelling of elastic deformation for initially anisotropic materials sustaining unilateral damage. Techn. Mech. 19, 211–222
36. **Fichant S, La Borderie C, Pijaudier-Cabot G** (1999) Isotropic and anisotropic descriptios of damage in concrete structures. Mech. Cohes.-Frict. Mater. 4, 339–359
37. **Lemaitre J, Desmorat L, Sauzay M** (2000) Anisotropic damage law of evolution. Eur. J. Mech. A/Solids 19, 187–208
38. **Zolochevskij AA** (1988) Kriechen von Konstruktionselementen aus Materialien mit von der Belastung abhängigen Charakteristiken. Techn. Mech. 9, 177–184
39. **Betten J, Sklepus S, Zolochevsky A** (1998) A creep damage model for initially isotropic materials with different properties in tension and compression. Eng. Fracture Mech. 59, 623–641
40. **Betten J, Sklepus S, Zolochevsky A** (1999) A microcrack description of creep damage in crystalline solids with different behaviour in tension and compression. Int. J. Damage Mech. 8, 197–232
41. **Betten J, Sklepus S, Zolochevsky A** (1999) Modeling of unilateral creep damage. Reports of the National Ukrainian Academy of Sciences (7), 53–57

42. **Voyiadjis GZ, Zolochevsky A** (2000) Thermodynamic modeling of creep damage in materials with different properties in tension and compression. Int. J. Solids Struct. 37, 3281–3303
43. **Zolochevsky A, Obataya Y** (2001) Tension-compression asymmetry of creep and unilateral creep damage in aluminum for isothermal and nonisothermal processes. JSME International Journal. Series A 44, 100–108
44. **Zolochevsky A, Sklepus S, Kozmin Yu, Kozmin A, Zolochevsky D, Betten J** (2004) Constitutive equations of creep under changing multiaxial stresses for materials with different behavior in tension and compression. Forschung Ingenieurwes 68: 182–196
45. **Zolochevsky A, Obataya Y, Betten J** (2000) Critical plane approach with two families of microcracks for modelling of unilateral fatigue damage. Forschung Ingenieurwes 66: 49–56
46. **Zolochevsky A, Itoh T, Obataya Y, Betten J** (2000) A continuum damage mechanics model with the strain-based approach to biaxial low cycle fatigue failure. Forschung Ingenieurwes 66: 67–73
47. **Ehlers W** (1995) A single-surface yield function for geomaterials. Archive Appl. Mech. 65, 246–259
48. **Karihaloo BL, Fu D** (1990) An anisotropic damage model for plain concrete. Eng. Fracture Mech. 35, 205–209
49. **Panyaev V** (1970) On deformations and fracture of semibrittle bodies, Ph.D. Thesis, Kyrgyz Academy of Science, Automatica Institute, Frunze